Chapter 4

A Survey of Elastic and Electromagnetic Properties of Near-Surface Soils

J. Carlos Santamarina[1], Victor A. Rinaldi[2], Dante Fratta[3], Katherine A. Klein[4], Yu-Hsing Wang[5], Gye Chun Cho[6], and Giovanni Cascante[7]

Introduction

The near-surface is covered with soil in most onshore and offshore locations. Soil characterization by sampling and in-situ testing techniques (e.g., cone penetration and pressure meters) faces unavoidable perturbation effects. On the other hand, low-power geophysical techniques cause no appreciable perturbation and provide an effective alternative for site assessment. In particular, near-surface site characterization using elastic and electromagnetic perturbations yields important information related to the soil mass, including the spatial distribution of materials, small-strain elastic properties and electromagnetic characteristics. In turn, geophysical measurements can be associated with soil parameters relevant to geotechnical engineering analysis and design.

This chapter presents information about elastic (small-strain) and electromagnetic properties of soils and their relations to soil parameters. The goal is to explain physical links between geophysical measurements and soil properties, emphasize global trends, and highlight variables that exert first-order effects. The chapter includes simple, yet robust, concepts and relations that can be readily used in designing measurement procedures and in data interpretation. The information in this chapter is structured resembling Chapter 3 of this volume by Knight and Endres. Comprehensive coverage of equations, trends, and behavior discussed herein can be found in Santamarina et al. (2001).

List of Symbols

Note: Subindices are described in parenthesis.

α	attenuation coefficient
Δl	distance between two locations
ΔV	velocity change between two different frequencies
ε_0	permittivity of free space, $\varepsilon_0 = 8.85 \times 10^{-12}\ C^2/(N{\cdot}m^2) = 8.85 \times 10^{-12}$ F/m
γ	shear strain (γ_{elas} elastic threshold strain)
γ	unit weight
κ	relative permittivity (κ^* complex, κ' real, κ'' imaginary)
λ	wavelength
μ	relative magnetic permeability (μ^*: complex; μ': real; μ'': imaginary; m: mixture)
μ_0	magnetic permeability of free space ($4\pi{\cdot}10^7$ H/m)
ν	Poisson's ratio
θ, β	fitting parameters in velocity-stress relation
θ_v	volumetric water content
ϕ	friction angle
Θ	surface conduction
ρ	mass density (fl: fluid; g: mineral that makes the grains; sus: suspension)
σ	electrical conductivity (eff: effective; el: electrolyte; fl: fluid)
σ	stress (σ': effective stress; v: vertical; h: horizontal; mean: mean in polarization plane)
τ_{ult}	shear strength
ω	angular frequency
B	bulk stiffness (sk: soil skeleton; g: mineral that makes grains; sus: suspension; fl: fluid)
c_o	speed of light in free space, $c_o = 3' \times 10^8$ m/s
D	damping ratio
e	void ratio
f	frequency (r: resonant frequency)
g	acceleration due to gravity ($g = 9.81$ m/s^2)
G	shear modulus (sk: soil skeleton)
H	magnetic field
K_o	ratio between horizontal and vertical effective stress in situ
M	constraint modulus
M	mass (t: total; w: water; s: solids)
n	porosity
PI	plasticity index
Q	quality factor (S: S-wave; P: P-wave; R: Rayleigh wave)
S_d	skin depth
S_G	specific gravity
S_r	degree of saturation
S_s	specific surface
t_{ads}	thickness of adsorbed water
TDS	total dissolved salts in mg/L
u	pore fluid pressure
V	volume (t: total; v: voids; a: air; w: water)
V	wave velocity (ph: phase; P: P-wave; S: S-wave; R: Rayleigh wave)
V_0	velocity at the relaxation frequency
v_{Fe}	volume fraction of ferromagnetic inclusions
w_g	gravitational water content
z_{probed}	probed depth

[1]Georgia Institute of Technology, Atlanta, GA 30332, USA. E-mail: carlos@ce.gatech.edu.

[2]Universidad Nacional de Córdoba, Córdoba 5000, Argentina. E-mail: vrinaldi@efn.uncor.edu.

[3]Louisiana State University, Baton Rouge, LA 70803, USA. E-mail: dfratta@lsu.edu.

[4]University of Toronto, Toronto, Ont., M5S 1A4, Canada. E-mail: klein@ecf.utoronto.ca.

[5]Hong Kong University of Science and Technology, Hong Kong. E-mail: ceyhwang@ust.hk.

[6]Korea Advanced Inst. of Science and Tech., Daejeon, South Korea. E-mail: gyechun@mail.kaist.ac.kr.

[7]University of Waterloo, Waterloo, Ont., N2L 3G8, Canada. E-mail: gcascant@uwaterloo.ca.

Soil Properties

Soils are composed of mineral grains and pore fluid (e.g., air, water, organics). The particulate nature of soils determines most soil characteristics. The constituents, grain size distribution, and spatial variability of a near-surface soil formation reflect its *formation history* (Mitchell, 1993). For example, glacial deposits are heterogeneous and are composed of a wide range of particle sizes. On the other hand, eolian and deltaic formations have narrow grain size distributions. Residual soils form in situ (are not transported), are finer near the surface becoming coarser with depth, and may exhibit some degree of cementation. Some soils present clear records of climatic fluctuations, such as varved clays which are composed of successive seasonal thin layers of silt and clay, rendering a soil with high anisotropy in its mechanical, conduction, and diffusion properties. Diagenetic effects after deposition can severely alter the properties of granular materials. In particular, light cementation can drastically increase the small-strain shear stiffness (increases more than two orders of magnitude are possible), even when changes in strength remain relatively small.

Particle size is a critical soil parameter: the smaller the particle size, the higher the surface area of the grain relative to its volume, and the more important surface-related forces (electrical, capillary, and drag) become relative to self-weight and skeletal forces. For near-surface conditions, surface-related forces gain relevance in submillimetric-sized particles, and a clear transition in behavior occurs between 10-μm and 100-μm particles.

The *particle shape* in millimetric and larger sized particles tends to be spherical or cubical (the short, intermediate, and long axes are approximately the same length). However, micro- and submicron-sized particles become increasingly more platy or rodlike.

The range in *packing density* and *porosity* of a soil is intimately related to the grain size distribution of the soil (e.g., well-graded materials render higher maximum densities) and the particle shape (e.g., platy particles produce a wider range of densities). For example, the porosity in mono-size spherical particles can range between n = 0.476, corresponding to cubic packing, and n = 0.260 for a face centered cubic packing. On the other hand, the porosity of kaolinite can range from n = 0.91 at the slurry-to-sediment transition (i.e., suspended to interacting particles), to $n \sim 0.02$ in shales (hence, density and porosity in clays are affected by stress history). Typical values for near-surface soil conditions, phase diagrams and relations among gravimetric and volumetric parameters are summarized in Table 1.

Three distinct mechanisms contribute to *anisotropy* in soils. First, inherent depositional fabric anisotropy results from the sedimentation of nonspherical grains (geometrical eccentricity as low as 1.1:1 is sufficient to cause significant elastic anisotropy). Second, stress anisotropy alters interparticle forces and contacts, and produces global fabric anisotropy. Third, soil layering, as in the case of varved clays. The first two components alone can render shear stiffness anisotropy in excess of 1.7:1.

The mechanical response of the granular skeleton is intimately related to the *strain level*. The transition between small and medium strains is the *elastic threshold strain*. When shear strains are smaller than the elastic threshold strain, the behavior of the soil is considered quasi-elastic, the skeletal stiffness is maximum, and the energy loss is minimum. The elastic threshold strain increases as the confining stress acting on the skeleton increases, decreases with increasing stiffness of the mineral that makes the particles, and increases with increasing specific surface of the soil (Table 1). Geophysical studies involve small-strain phenomena.

The small-strain *stiffness* of the granular skeleton is determined by the flatness of interparticle contacts. Flatter contacts result from elastic, viscous, and/or plastic deformation of contacts in relation to interparticle forces (skeletal as well as capillary), and the precipitation of cementing species (including solution/precipitation of the grain mineral itself). Angular and rough particles lead to lower small-strain skeletal stiffness.

The most common *pore fluids* in near-surface soils are air and water. Organic fluids may be present as well, and are most often considered contaminants. The distinct properties of these fluids play a critical role in the application of elastic and electromagnetic waves for the characterization of near-surface formations:

- Air: low mass and high compressibility (yet, both effects combine to render a high sound velocity, V_P = 343 m/s, which is higher than the velocity of elastic waves in most near-surface soils), dielectric permittivity similar to free space, and very limited electrical conductivity.
- Water: high bulk stiffness; composed of polar water molecules, thus, it hydrates salts forming electrolytes, and hydrates ions adsorbed on mineral surfaces rendering double layers; high interfacial tension with either air or immiscible organic fluids.
- Organic fluids (contaminants): high bulk stiffness, mostly nonpolar.
- De-aired liquids are characterized by a high bulk stiffness, which exceeds the bulk stiffness of the granular skeleton for near-surface soils. The presence of air causes a very drastic drop in the bulk stiffness of fluids and creates mixed-fluid conditions.

In the presence of fluids, the total boundary stress σ applied to a soil mass is shared by the granular skeleton and the fluid[8]. The portion carried by the skeleton is the *effective stress* σ'. For near-surface soils, the bulk stiffness

[8]The symbol σ is later used for electrical conductivity. The meaning of σ is evident by context.

Table 1. Phase relations, porosity, and threshold strain.

Phase diagram

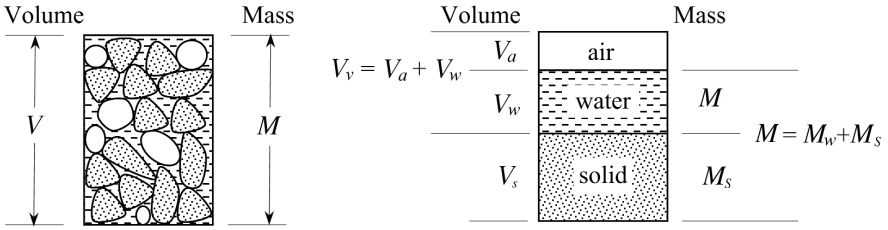

Mass density: $\rho = \frac{M}{V}$

Unit weight: $\gamma = \rho g$

Void ratio: $e = \frac{V_v}{V_S} = \frac{n}{1-n}$

Porosity: $n = \frac{V_v}{V} = \frac{e}{1+e}$

Degree of saturation: $S_r = \frac{V_W}{V_v}$

Specific surface: $S_S = \frac{\text{surface area}}{\text{mass}}$

Grav. water content: $W_g = \frac{W_W}{W_S}$

Vol. water content: $\theta_v = \frac{V_W}{V} = nS_r = \frac{S_G W_g}{1+e}$

Specific gravity: $S_G = \frac{\rho_g}{\rho_W}$

Useful relation: $S_r e = S_G W_g$

Grav. water content for adsorbed water thickness t_{ads}: $W_g = S_S t_{ads} \rho_W$

Typical porosity and specific surface values for near-surface soils

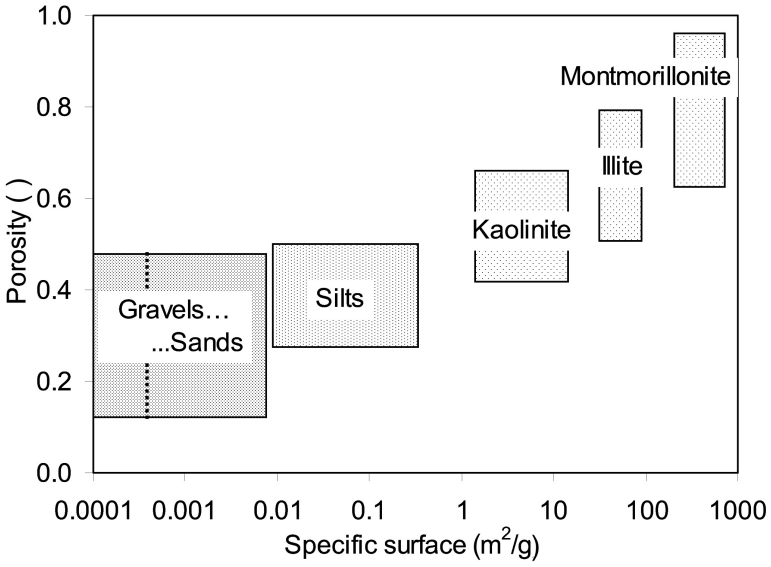

Elastic threshold shear strain γ_{elas}

Increases with effective confinement and with soil plasticity (fineness)

Low end: $\gamma_{elas} = 5 \times 10^{-6}$ (e.g., sand at 20 kPa confinement)

High end: $\gamma_{elas} = 1 \times 10^{-4}$ (e.g., kaolinite at 200 kPa confinement)

Additional information: Lanzo and Vucetic (1999); Diaz-Rodriguez and Santamarina (2001).

of the skeleton B_{sk} is much smaller than the bulk stiffness of the mineral that makes the grains B_g; in this case, the effective stress σ' is equal to the total stress σ minus the pore fluid pressure u,

$$\sigma' = \sigma - u. \quad (1)$$

The effective stress determines shear strength τ_{ult} (e.g., Coulomb's failure criterion: $\tau_{ult} = \sigma' \tan \phi$ where ϕ is the friction angle of the soil), stiffness (e.g., Hertzian behavior), and dilatancy (i.e., the volume change upon shear may be either positive or negative).

The presence of *two nonmiscible fluids* adds interfacial tension and *capillary forces* between particles. This is typically the case between air and water, or water and organic fluids. One or both fluids may percolate; the one that percolates controls the global electrical conductivity. Saturation conditions often vary in the near-surface. Typically, the formation is water-saturated below the water table; above the water table, the *degree of saturation* S_r decreases towards the free surface. The effect of capillary forces on soil behavior increases as particle size decreases, and should be taken into consideration in clayey or silty soils.

Given the dipolar nature of water molecules and their thermal vibration, water effectively dissolves excess salts present in the soil, hydrates ions adsorbed on mineral surfaces, and may dissolve the mineral itself depending on pH and the type and concentration of hydrated ions. The immediate consequences of these phenomena include

- The pore water in any soil is an *aqueous electrolyte*, that is, it consists of free water molecules and hydrated cations and anions that can move relative to each other.
- Hydrated counter-ions around mineral surfaces gain mobility, yet they remain in the vicinity of the particle surface due to Coulombian attraction (i.e., to satisfy electroneutrality), forming a *diffuse layer*.
- The resulting counter-ion cloud interacts with the cloud around neighboring particles leading to the development of interparticle *electrical forces*. These forces can affect the mechanical behavior of near-surface clayey soils.

Main observations

The previous discussion introduced the multiple microscale phenomena that coexist in soils and the ensuing macroscale properties. The principal observations in view of elastic and electromagnetic properties follow:

- The granular skeleton of a soil is composed of interacting mineral particles.
- The soil mass is not inert and its properties are not constant.
- The granular skeleton is inherently porous and pervious.
- The pore volume is filled with the fluid phase, which can be air, water, organic contaminants, or mixtures thereof.
- The mechanical response (stiffness, shear strength, volume change) of the granular skeleton that makes the soil is determined by the effective stress.
- When particles are small, the specific surface is high and surface related forces gain relevance relative to interparticle forces transmitted through the granular skeleton.
- In particular, electrical and capillary forces should be considered when particles are smaller than ~10 μm. In this case, changes in the state of stress, degree of saturation and/or fluid chemistry cause changes in the soil response.

Wave Phenomena and Soils

Near-surface soil characterization using elastic and electromagnetic waves involves long-wavelength conditions, whereby the wavelength is much longer than the particle size. The two types of waves experience similar wave phenomena, including time delay, attenuation, dispersion, reflection, refraction, diffraction, and interference. A list of salient wave phenomena and differences between elastic and electromagnetic waves are presented in Table 2.

Such multiplicity of possible wave phenomena hints at the complexity of wave-based studies. More importantly, it also highlights the potential for gaining detailed information about the medium by explicitly targeting these phenomena. In general, properly designed test procedures and adequate signal processing are required.

The propagation velocity and attenuation of mechanical and electromagnetic perturbations in soils depend on distinct soil properties. Elastic wave propagation is affected by soil parameters that determine mass density ρ, and the complex bulk stiffness B and shear stiffness G. On the other hand, the propagation of electromagnetic waves is affected by soil properties that determine polarizability, electrical conductivity, and magnetizability. These interrelations are explored in the following sections.

Elastic Properties of Soils

Near-surface characterization using elastic waves is conducted at frequencies that vary between a few Hz to a few kHz. In this frequency range, the wavelength in soils ranges between tens of centimeters to tens of meters, therefore, the wavelength is much greater than the grain size, and the perturbation propagates through the soil mass as in a continuum.

The propagation of elastic waves in geophysical studies involves strain levels that are lower than the threshold strain of the soil (Table 1—Exception: sources of mechanical waves tend to cause large local amplitude, and emitted

waves experience high attenuation in the near field of the source). Then, relevant equations for velocity, attenuation, and dispersion in soils can be obtained by presuming viscoelastic wave propagation conditions. These concepts and relations are summarized next.

Wave velocity

There are three important propagation modes in the near-surface: longitudinal P-waves, transverse S-waves, and retrograde elliptical Rayleigh R-waves. The propagation velocity in each mode and the controlling soil variables are discussed next.

P-waves and S-waves

The shear modulus of the soil G_{soil} only depends on the skeleton shear stiffness, $G_{\text{soil}} = G_{sk}$, and it is not affected by the bulk stiffness of the pore fluid. For this reason, S-waves are preferred for the characterization of near-surface deposits when the soil mass is saturated. The shear-wave velocity V_S is

$$V_S = \sqrt{\frac{G_{\text{soil}}}{\rho_{\text{soil}}}}, \tag{2}$$

where ρ_{soil} is the mass density of the soil mass. The shear modulus of soils is determined by the state of stress, the

Table 2. Wave phenomena in the near surface.

Media characteristics	Phenomena (both waves)	Special manifestations in elastic or electromagnetic waves	
Interfaces and boundaries	Reflection Refraction Dispersion	Mec EM	Mode conversion Rayleigh, Love, Stonley waves Polarization-dependent reflect. Brewster's angles of total trans.
Anisotropy	Birefringence	Mec EM	S-wave splitting Quasi-propagation Birefringence
Gradual variation in depth (velocity gradient)	Ray bending	Mec	R-wave dispersion
Inclusions—anomalies (e.g., λ versus size)	Diffraction Scattering Low-pass filtering		
Material spatial scales (e.g., λ versus layer thickness)	Low-pass filtering Multiple layer reflections		
Material time scales (e.g., ω versus relaxation time)	Attenuation Dispersion Resonance		
Multiphase	Attenuation Dispersion	Mec EM	Relaxation Biot slow P-wave Multiple relaxations
Nonlinear behavior (i.e., excitation exceeds linear threshold)	High loss	Mec EM	Shock-waves Heating, sparks
Inherent coupling between electrical, mechanical, chemical, and thermal energies	Dynamic energy coupling	Mec EM	Seismoelectric Electroseismic

Note: Elastic ("Mec") or Electromagnetic ("EM") waves.

degree of cementation, and by processes that alter interparticle contacts such as capillary forces and electrical forces. Shear-wave velocity values can be lower than 1 m/s for soils near the suspension-to-skeleton transition, and can reach 300 m/s to 400 m/s at depths of about 40 m. Cementation, even when light, can drastically increase the shear-wave velocity, reaching and exceeding 700 m/s. High suction in unsaturated fine grained soils can have a similar effect. Table 3 presents additional guidelines for the estimation of shear-wave velocity.

The propagation velocity of longitudinal P-waves is proportional to the constraint modulus M and the mass density ρ of the soil mass:

$$V_P = \sqrt{\frac{M_{\text{soil}}}{\rho_{\text{soil}}}} = \sqrt{\frac{B_{\text{soil}} + \frac{4}{3} G_{\text{soil}}}{\rho_{\text{soil}}}}, \tag{3}$$

where B_{soil} is the bulk modulus and G_{soil} is the shear modulus of the soil. The bulk stiffness of the minerals that make the grains B_g is much greater than the bulk stiffness of the granular skeleton B_{sk} (in this case, Biot-Gassman relations can be simplified; in fact, the Biot relaxation in soils is small for most practical purposes). Furthermore, the bulk stiffness of de-aired fluids $B_{\text{fl}} = B_w$ is also greater than the bulk stiffness of the skeleton. However, even minute quantities of air in the fluid phase drastically reduce the bulk modulus of the fluid mixture. Expressions for the bulk modulus of the soil B_{soil} as a function of the bulk modulus of fluid B_{fl} and the particles B_g, the degree of saturation S_r, and the porosity n of the soil are presented in Table 3.

Rayleigh waves

The free soil-air or sediment-water boundary promotes the formation of surface R-waves. The Rayleigh wave velocity V_R is related to the S-wave and P-wave velocities, and can be estimated as (modified from Achenbach, 1975)

$$V_R \approx \frac{0.874 + 1.117\,\nu}{1+\nu} V_S, \tag{4}$$

where ν is Poisson's ratio. For unsaturated soils, $V_R \approx 0.9\,V_S$. R-waves permit characterizing the near-surface without drilling boreholes. The depth probed by the perturbation is proportional to the wavelength $z_{\text{probed}} \approx \lambda = V_R / f$. R-wave propagation is nondispersive in homogeneous materials. However, when the medium is heterogeneous, all layers within the probed depth z_{probed} affect the propagation velocity at a given frequency. Therefore, the velocity is not constant with frequency, and the measured velocity-frequency dispersion curve can be inverted to infer the variation of the medium with depth; the technique is known as spectral analysis of surface waves or SASW (Gucunski and Woods, 1992; Stokoe et al., 1994; Tokimatsu, 1995; Miller et al. 1999, Rix et al., 2002).

Poisson's ratio

The small-strain value of Poisson's ratio ν can be estimated from V_P and V_S velocities,

$$\nu = \frac{\frac{1}{2}\left(\frac{V_P}{V_S}\right)^2 - 1}{\left(\frac{V_P}{V_S}\right)^2 - 1}, \tag{5}$$

The Poisson's ratio for saturated soft soils (S_r = 100%) approaches $\nu \rightarrow 0.5$. The small-strain Poisson's ratio for unsaturated soils (S_r < 99%) is lower than ν < ~0.15.

Material attenuation

The amplitude of propagating waves decreases with distance. This is due to geometric spreading of the wavefront, partial transmission at interfaces, and material losses. In the absence of geometric spreading, the amplitudes A_1 and A_2 of a plane wave at two locations Δl apart in a quasi-homogeneous medium, are related by the material attenuation coefficient α [m^{-1}], $A_2/A_1 = e^{(-\alpha \Delta l)}$. The attenuation coefficient α for elastic waves in soils can be related to other measures of energy loss, including the quality factor Q and the damping ratio D,

$$\frac{1}{Q} = \frac{V\alpha}{\pi f} = 2D. \tag{6}$$

In terms of the damping ratio D, soils are highly underdamped materials (D << 100%). The small-strain damping ratio for oven-dry sands captures thermo-elastic effects and can be smaller than D < 0.2% (Q > 250). In moist and saturated soils, energy losses are governed by viscous effects, and the damping ratio can reach values of D = 2% to 5% (Q = 25 to 10). The damping ratio $D = 1/(2Q)$ is constant in dry soils and it increases linearly with frequency in wet soils. Additional values and trends are summarized in Table 4.

The "skin depth" S_d is the distance the wave travels before its amplitude decays by $1/e$. Therefore, the skin depth for a plane wave is $1/\alpha$. It follows from equation (6) that the skin depth S_d is

$$S_d = \frac{1}{\alpha} = \lambda \frac{Q}{\pi} = \lambda \frac{1}{2\pi D}. \tag{7}$$

Therefore, for the range of damping in soils, typically between D ~ 0.1% (i.e., Q ~ 500) and D < 5% (i.e., Q > 10), the skin depth for elastic waves is many times the wavelength. This is an important advantage for the characterization of near-surface soils.

Table 3. Wave velocity in soils.

Physical processes

effective stress

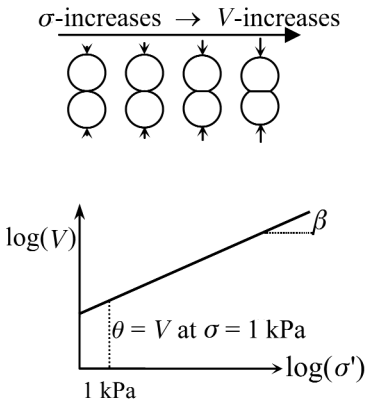

Cementation:

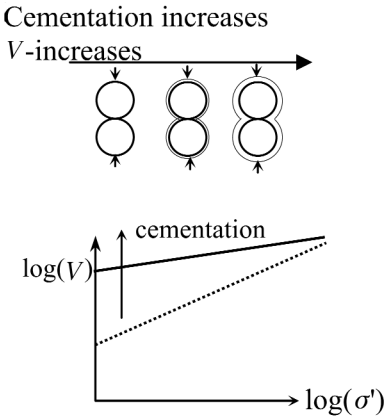

Partial saturation

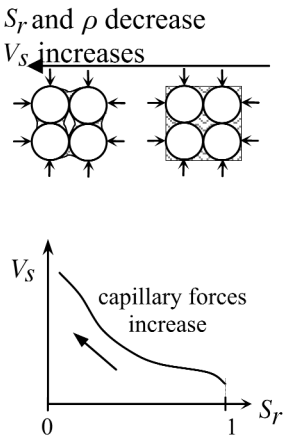

Shear-wave velocity V_S
(Saturated or dry soils)

$$V_S = \theta\left(\frac{\sigma'_{mean}}{1\,kPa}\right)^{\beta}$$

σ'_{mean} mean effective stress on polarization plane

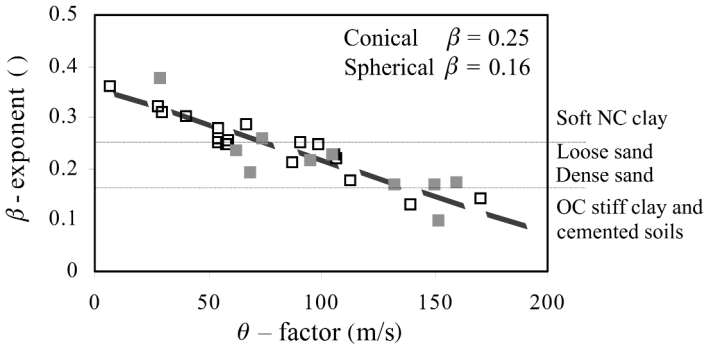

Unsaturated soils—Capillary effects on V_S [1]

The finer the soil and the lower the water content, the higher the suction. At S_r = 100%, suction = 0

$$V_S \approx V_{S\,(\text{for } S_r=1.0)}\left[1+\frac{\text{suction}\times S_r}{0.75\,\sigma'_v}\right]^{\beta}$$

Bulk modulus and mass density [2]

Fluid mixture	$B_{fl}=\left(\frac{S_r}{B_w}+\frac{1-S_r}{B_a}\right)^{-1}$	$\rho_{fl}=(1-S_r)\rho_a+S_r\rho_w$ $\rho_{fl}=S_r\rho_w$ in case a ≡ air
Suspension (fluid + particles)	$B_{sus}=\left(\frac{1-n}{B_g}+\frac{n}{B_{fl}}\right)^{-1}$	$\rho_{sus}=(1-n)\rho_g+n\rho_{fl}$
Soil (fluid + skeleton)	$B_{soil}=B_{sus}+B_{sk}$	$\rho_{soil}=\rho_{sus}=(1-n)\rho_g+n\rho_{fl}$

Typical values in m/s (top 40 m)

V_P in water	1482	V_P in air	343
V_P in saturated soils	1450–1900	V_S in saturated soils	<50–400
V_P in unsaturated soils	<100–800	V_S in unsaturated clayey soils	<100–500
V_P in lightly cemented soils	400–1000	V_S in lightly cemented soils	250–700

Note: [1]For the measurement of suction, see Fredlund and Rahardjo (1993). [2]Assumes $B_{sk}/B_g \approx 0$ and low-frequency limit.

Sources: Richart et al. (1970); Hardin and Drnevich (1972); Reynolds (1997); Santamarina et al. (2001); Cho and Santamarina (2001).

Table 4. Elastic wave attenuation in soils.

Physical processes				
Dry—small strain:	thermo-elastic relaxation			
Moist/wet—small strain:	viscous loss prevails			
Large strain:	frictional loss			
Surface waves				
(White, 1983)	$\frac{Q_S}{Q_R} = \frac{\frac{Q_S}{Q_P}\left[4(1-a)\frac{b}{a}\right] + 4(1-b) - (2-a)^3}{\left[4(1-a)\frac{b}{a}\right] + 4(1-b) - (2-a)^3}$	$a = (V_R/V_S)^2,\ b = (V_R/V_P)^2$		
Typical damping values at small strain				
Gravelly Soils	D = 0.008 – 0.018	σ_0' = 100 – 400 kPa	$\gamma < 10^{-5}$	CT
Sand	D = 0.002 – 0.01	σ_0' = 20 – 1800 kPa	$\gamma < 10^{-5}$	RC
Air-dry				
Saturated	D = 0.003 – 0.021	σ_0' = 28 – 1800 kPa	$\gamma = 10^{-5}$	CT and RC
Clayey soils	D = 0.01 – 0.052	σ_0' = 15 – 500 kPa	$\gamma < 10^{-4}$	CT and RC
Residual soils	D = 0.009 – 0.054	σ_0' = 25 – 35 kPa	$\gamma < 10^{-5}$	RC
Peat ($w_g \approx 200\%$)	$D \approx 0.025$	σ_0' = 66 – 135 kPa	$\gamma \approx 10^{-5}$	CT

Notes: γ is the strain, σ_0' is the effective confinement, w_g is the gravimetric water content, and PI is the plasticity index. RC: resonant column test (typical frequency range 50 Hz to 250 Hz). CT: cyclic triaxial test (typical frequency range <1 Hz).

Sources: Yasuda and Matsumoto (1993); Kim et al. (1991); Laird and Stokoe (1993); Santamarina and Cascante (1996); Li et al. (1998); Kokusho (1980); Kokusho et al. (1982); Cascante and Santamarina (1996); Diaz-Rodriguez and Santamarina (2001); Kim and Novak (1981).

Attenuation-dispersion

Nearly constant and constant damping models predict an increase in velocity of about 1.5 D for a ten-fold increase in frequency (e.g., Kjartansson, 1979). For example, given a soil with damping ratio D = 1%, the velocity increase for a log-cycle in frequency is about 1.5%.

In the case of visco-elastic losses, the maximum attenuation takes place at the relaxation frequency, and it is related to the normalized change in velocity across the relaxation, 2 $D_{max} = \Delta V/V_o$. For example, if the velocity changes 6% across the relaxation, the maximum damping will be about D_{max} = 3%. Most of the change in velocity takes place within one log cycle before and after the relaxation frequency. (Note: high-frequency excitation at kHz-frequencies are still much lower than Biot's critical frequency for most soils, which is estimated in the kHz for coarse clean sands and in the MHz for clays).

Main observations—Example

Equations, data, and trends in this section and in Tables 3 and 4 support the following main observations about elastic-wave propagation in near-surface soils:

- If the *soil is saturated* with de-aired water (S_r = 100%), the P-wave velocity of the soil varies between ~1450 m/s and about ~1900 m/s (depending on porosity n), Poisson's ratio approaches $v \rightarrow 0.5$, and the shear-wave velocity is determined by the shear stiffness of the soil skeleton (and the mass density of the soil).
- If the *soil is unsaturated* ($S_r < 99.0\%$), the bulk stiffness of the fluid is very low, the bulk and shear moduli of the soil mass are those of the soil skeleton, Poisson's ratio is low $v < 0.15$, and the P-wave velocity is about 1.4 to 1.6 times higher than the shear-wave velocity.

- The velocity of S-waves for any degree of saturation and the velocity of P-waves in unsaturated soils ($S_r < 99\%$) are determined by (1) cementation—even light cementation can increase velocity by several times; (2) state of effective stress in uncemented soils; (3) capillary forces in silty or clayey soils (depends on particle size and degree of saturation); and (4) other effects such as those that control mass density or that may alter interparticle electrical forces.
- The wave velocity is approximately constant in all soils for frequencies below a few kHz. Velocity variations are on the order of a few percentage points per log cycle of frequency.
- The dispersion of surface waves captures the variability of the soil profile.
- Attenuation is low, rendering damping ratio values between $D \sim 0.1\%$ (i.e., $Q \sim 500$) and $D < 5\%$ (i.e., $Q > 10$). The skin depth is many times greater than the wavelength.

The application of equations and trends introduced in this section is illustrated in Example 1.

Electromagnetic Parameters

The electromagnetic properties of geomaterials include the magnetic permeability μ (the ability of the medium to respond to a magnetic field), the dielectric permittivity κ (the ability of the soil to become polarized in response to an electric field), and the conductivity σ (the availability and mobility of charges). Both relative permittivity and relative permeability are complex quantities κ^* and μ^* (Chapter 3),

$$\mu^* = \mu' - j\mu'' \tag{8}$$

and

$$\kappa^* = \kappa' - j\kappa''. \tag{9}$$

The imaginary components μ'' and κ'' capture magnetization and polarization losses, respectively. These components are in phase with the conductivity, rendering an effective conductivity that increases with frequency:

$$\sigma_{\text{eff}} = \kappa'\mu''\varepsilon_0\omega + \left(\sigma + \kappa''\varepsilon_0\omega\right)\mu'. \tag{10}$$

A propagating electromagnetic wave travels through the soil with phase velocity V_{ph}:

$$V_{ph} = \frac{c_0}{\text{Im}\left[\sqrt{\left(-\kappa'\mu' + \kappa''\mu'' + \frac{\sigma\mu''}{\varepsilon_0\omega}\right) + j\left(\frac{\sigma_{\text{eff}}}{\varepsilon_0\omega}\right)}\right]}, \tag{11}$$

where $c_0 = 2.99 \times 10^8$ m/s is the speed of light in free space. The attenuation coefficient α is

$$\alpha = \frac{\omega}{c_0}\text{Re}\left[\sqrt{\left(-\kappa'\mu' + \kappa''\mu'' + \frac{\sigma\mu''}{\varepsilon_0\omega}\right) + j\left(\frac{\sigma_{\text{eff}}}{\varepsilon_0\omega}\right)}\right]. \tag{12}$$

Most soils in the near-surface are nonferromagnetic ($\mu' = 1$ and $\mu'' = 0$). In this case, the previous equations become,

$$\sigma_{\text{eff}} = \sigma + \kappa''\varepsilon_0\omega, \tag{13}$$

$$V_{ph} = \frac{c_0}{\sqrt{\kappa'}} \cdot \frac{1}{\sqrt{\frac{1}{2}\left(\sqrt{1 + \left(\frac{\sigma_{\text{eff}}}{\varepsilon_0\omega\kappa'}\right)^2} + 1\right)}}, \tag{14}$$

and

$$\alpha = \frac{\omega\sqrt{\kappa'}}{c_0}\sqrt{\frac{1}{2}\left(\sqrt{1 + \left(\frac{\sigma_{\text{eff}}}{\varepsilon_0\omega\kappa'}\right)^2} - 1\right)}. \tag{15}$$

Although elastic-wave propagation in soils always involves low-loss conditions, this may not be the case for electromagnetic waves. In many cases, the effective conductivity of the soil is high and the skin depth $S_d = 1/\alpha$ is smaller than the wavelength. When the effective conductivity is small $\sigma_{\text{eff}}/(\varepsilon_0\omega\kappa') << 1$, the skin depth is many times the wavelength and the phase velocity becomes $V_{ph} = c_0/\sqrt{\kappa'}$.

These equations show that velocity and attenuation vary with frequency for a given set of material properties. Furthermore, the electromagnetic properties of soils are frequency-dependent themselves. The following discussion of electromagnetic properties provides a physical explanation in the case of soils, and guidelines for their estimation and interpretation. The discussion is centered on frequency ranges that are compatible with the operating frequencies of the most common geophysical techniques for near-surface characterization as listed next.

Magnetic permeability

Water and most soil-forming minerals are nonferromagnetic (i.e., the real relative magnetic permeability is about $\mu' \approx 1$). When ferromagnetic impurities are present, the magnetic permeability of the soil mass is proportional to the volume fraction of impurities. Such mixtures may present relaxation spectra in the kHz range. Typical values of magnetic permeability and an expression for the mixture of clay and a low-volume fraction of iron-filings are presented in Table 5.

Example 1. Elastic wave-parameter estimation

Consider a saturated (S_r = 1.0) sandy soil with porosity n = 0.35 (Table 1). The assumed specific gravity and bulk stiffness of the mineral that makes the grains are S_G = 2.65 and $B_g = 3.5 \times 10^{12}$ N/m^2. The water table is at a depth z_w = 2 m. Estimate elastic wave propagation conditions at a depth of z = 10 m for a high-resolution near-surface study conducted at a frequency f ~ 800 Hz.

Preliminary computations

Table 1: $e = n/(1\text{-}n) = 0.54$

Table 1: $\rho_g = S_G \times \rho_w = 2650$ kg/m^3

Table 3: $\rho_{soil} = (1\text{-n})\rho_g = 1722$ kg/m^3 — above water table (assumed dry)

$\rho_{soil} = (1\text{-n})\rho_g + \text{n}(S_r \times \rho_w) = 2072$ kg/m^3 — below water table (assumed saturated)

State of stress σ′ at z = 10 m (g = 9.81 m/s^2 is the acceleration of gravity)

$\sigma_v = \Sigma z \times \rho_{soil} \times g = 2\ (1722\ \text{kg/m}^3) \times \text{g} + 8\ (2072\ \text{kg/m}^3) \times \text{g} = 196.4$ kPa

$u = z \times \rho_w \times \text{g} = 8\ (1000\ \text{kg/m}^3) \times g = 78.5$ kPa

Equation 1: $\sigma'_v = \sigma_v - n = 196.4\ \text{kPa} - 78.5\ \text{kPa} = 117.9$ kPa

Ratio of effective stresses at rest $K_o \approx 0.5$ (estimated)

$\sigma'_h = K_o \times \sigma'_v = 0.5 \times 117.9\ \text{kPa} = 59$ kPa

$\sigma'_{mean} = (\sigma'_v + \sigma'_h)/2 = (117.9\ \text{kPa} + 59\ \text{kPa})/2 = 88.4$ kPa

S-wave velocity at z = 10 m (for S_{HV}, i.e., polarized on the vertical plane)

Table 3: $\beta = 0.22$ $\theta = 80$ m/s (for loose to dense sand)

Table 3: $V_S = \theta(\sigma'_{mean}/1\ \text{kPa})^{\beta} = 80\ \text{m/s}\ (88.4\ \text{kPa}/1\ \text{kPa})^{0.22} = 214.5$ m/s

Velocity within range listed in Table 3

P-wave velocity at z = 10 m

Equation 2: $G_{soil} = V_S^2 \times \rho_{soil} = (228.5\ \text{m/s})^2 \times 2072\ \text{kg/m}^3 = 1.1 \times 10^5$ kPa

$B_{sk} = (2/3)G_{soil}(1+\nu)/(1\text{-}2\nu) = 8.7 \times 10^4$ kPa

Table 3: $B_{sus} = [n/B_w + (1\text{-n})/B_g]^{-1} = 5.41 \times 10^6$ kPa

Table 3: $B_{soil} = B_{sus} + B_{sk} = 5.5 \times 10^6$ kPa

Equation 3: $V_P = [(B_{soil} + 4/3 \times G_{soil})/\rho_{soil}]^{0.5} = 1648$ m/s

Velocity within range listed in Table 3

Damping

Table 4: Expect damping D ~ 0.01-0.02 (with some increase with frequency)

Wavelength and skin depth (considering D ~ 0.02 for both P and S-waves)

S-wave wavelength: $\lambda = V_S/f = 214.5\ \text{m/s} / 800\ \text{Hz} = 0.27$ m

skin depth: $S_d = \lambda/(2\pi D) = 0.27\ \text{m} / (2\pi \times 0.02) = 2.13$ m

P-wave wavelength: $\lambda = V_P/f = 1648\ \text{m/s} / 800\ \text{Hz} = 2.06$ m

skin depth: $S_d = \lambda/(2\pi D) = 1080\ \text{m} / (2\pi \times 0.02) = 16.39$ m

Table 5. Magnetic permeability.

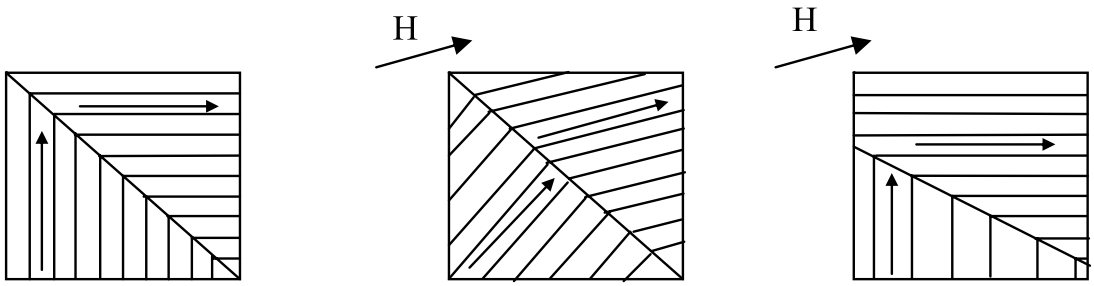

Magnetization mechanisms in ferromagnetic materials: (a) no magnetic field $H = 0$; (b) rotation of spins within domains $H > 0$; and (c) translation of domain walls $H > 0$.

Single materials	
Water, quartz, kaolinite	~0.9999 (diamagnetic)
Montmorillonite, illite, granite, hematite	1.00002–1.0005 (paramagnetic)
Nickel, iron	> 300 (ferromagnetic)
Predictive relations	
Wagner's model for spherical particles[1]	$\mu' = 1 + 3v_{Fe}$ for $v_{Fe} < 0.2$
Kaolinite with iron filings (at 10 kHz)[2]	$\mu' = 1 + 4v_{Fe} + 7v_{Fe}^2$ for $v_{Fe} < 0.3$

Sources: [1]Göktürk et al. (1993); [2]Klein and Santamarina (2000).
Note: v_{Fe} is the volume fraction of ferromagnetic inclusions.

Dielectric permittivity (relevant frequency range: MHz)

Soils are electrically neutral overall; however, negative charges (electrons and anions) and positive charges (protons and cations) can be displaced by applying an electric field. When charges are displaced from their equilibrium position, the medium becomes polarized. The permittivity of a material increases from high frequencies to low frequencies, gradually accumulating polarizations as the frequency decreases and larger scales become involved. The following observations and trends apply to geomaterials at MHz frequencies:

- The permittivity of most soil-forming minerals ranges between 3 and 10. The permittivity of free water below $f < 10$ GHz is about 80.
- Given the high porosity of near-surface soils, the measured permittivity in soils at $f > 200$ MHz is dominated by the orientation polarization of free water (water beyond the adsorbed water layer around particles of thickness $t_{ads} \approx 2$–3 monolayers—Table 1). In this frequency range, the permittivity is controlled by the *volumetric* water content. Hence, if the soil is saturated, the porosity can be determined.
- The displacement of hydrated ions in the pore fluid and in double layers is restricted by interfaces (e.g., the particles themselves); this adds interfacial polarization at low MHz frequencies. Therefore, the permittivity at frequencies lower than ~100 MHz depends not only on volumetric water content, but also on the ionic concentration of the pore fluid, the specific surface of the soil, and the interparticle arrangement.
- The prevalence of Ohmic losses at frequencies lower than ~10 MHz causes high attenuation in wave propagation and the skin depth is shorter than the wavelength.

Table 6 provides typical values and convenient trends for soils.

Electrical conductivity (relevant frequency range: Hz-to-kHz)

The electrical conductivity of most soil-forming minerals as well as the conductivity of deionized water are very low ($\sigma < 10^{-4}$ S/m). However, the mixture of water and soils can exhibit high electrical conductivity. There are two participating phenomena:

- Water hydrates excess salts and the pore fluid becomes

Table 6. Permittivity (relevant frequency range 1 MHz–1 GHz).

Polarization

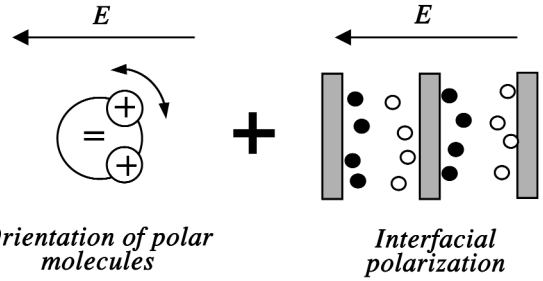

Note: Permittivity increases as frequency decreases.

Permittivity of single-phase soil components (radio frequencies)

Water	78.5	Quartz	4.2–5
Methanol	32.6	Calcite	7.7–8.5
Most organic fluids	2–6	Most minerals	6–10

Permittivity of wet soils ($\theta_v = S_r \times n$)	Frequency	Reference
$\kappa' = 1.40 + 87.6\,\theta_v - 18.7\,\theta_v^2$	50 MHz	Wensink (1993)
$\kappa' = 3.03 + 9.3\theta_v + 146.0\theta_v^2 - 76.7\,\theta_v^3$	MHz to GHz	Topp et al. (1980)
$\kappa' = 3.3 + 41.4\theta_v + 16.0\theta_v^2$	~ 1GHz	Wensink (1993)
$\kappa' = 3.14 + 23.8\theta_v + 16.0\theta_v^2$		Wang (1980)
$\kappa' = 40\theta_v - 3.9 + \sqrt{44.8 - 392\theta_v + 1600\theta_v^2}$		Selig and Mansukhani (1975)
$\kappa' = (2.6 - 1.6\,\mathrm{n} + 7.9\theta_v)^2$		Based on CRI mixture model

Trend for soils (f ~ 1 GHz)

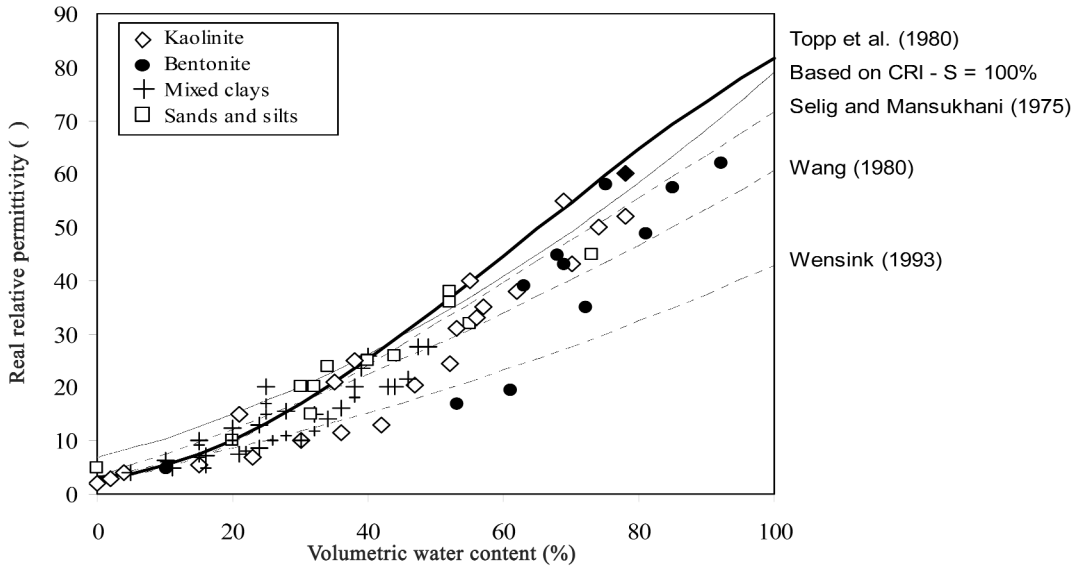

Data: unpublished data by the authors; Peplinski et al. (1995); Saarenketa (1998); Arulanandan (1991); Olhoeft, (1981); Parkhomenko (1967).

an electrolyte, that is, a mixture of free water molecules, hydrated cations and hydrated anions.

- Water also hydrates counter-ions adsorbed onto dry particles, thereby forming a counter-ion cloud around the particle.

Therefore, the electrical conductivity in soils is ionic in nature and includes contributions from (1) the pore fluid electrolyte (but reduced by the porosity, saturation, and tortuosity); and (2) the conduction along the particle surfaces, which is proportional to the specific surface of the soil. The contribution of surface conduction to the global conduction gains relevance in clays filled with a low-conductivity electrolyte. Trends and characteristic values are presented in Table 7.

Table 7. Electrical conductivity.

Availability and mobility of hydrated ions

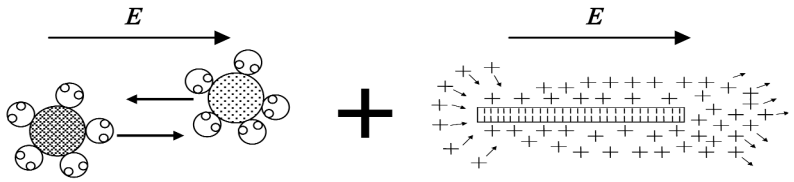

Hydrated ion mobility *Double layer surface conduction*

Note: The effective conductivity increases as frequency increases.

Conductivity of single-phase soil components (σ in S/m)

Deionized water	10^{-6}	Organic fluids	$\sim 10^{-11}$
Fresh water	10^{-3}	Most soil-forming minerals	10^{-15}–10^{-7}
Seawater	4	(Note: Some minerals are conductive.)	

Medium	Value—Trend	Comments
Water + salt = electrolyte	$\sigma_{el} = 0.15$ TDS	σ_{el} in mS/m; TDS: total dissolved salts in mg/L (Annan, 1992)
Wet soils	$\sigma_{\text{soil}} = n\sigma_{el} = (1 - n)\ \Theta\ \rho_g S_s$	Θ is surface conduction. Needs correction for tortuosity and saturation (see also O'Konski, 1960).
	$\sigma_{\text{soil}} = a\sigma_{el} S_s^c\, n^m$	$a \approx 1$ $m \sim 1$–2.4 $c \sim 4$–5 (Archie, 1942)

Trend for soils (σ in S/m)

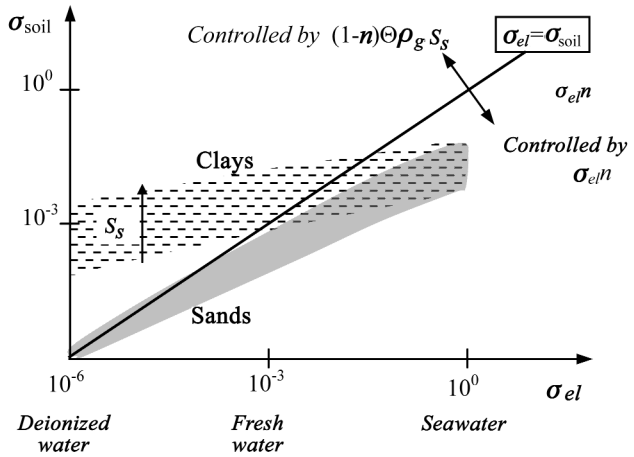

Notes: The surface conduction for kaolinite is about $\Theta \approx 10^{-9}$ Siemens. Tortuosity may reduce the electrical conductivity in clays more than in sands. Hence, the conductivity of marine clays may be lower than the conductivity of marine sands, at the same void ratio.

Sources: Annan (1992); Reynolds (1997); Santamarina et al. (2001).

Main observations—Example

There are three material properties that affect the propagation of electromagnetic waves in soils: magnetic permeability, permittivity, and electrical conductivity. The information presented in this section and in Tables 5, 6, and 7 permit extracting the following main conclusions:

- The magnetic permeability increases as the amount of ferromagnetic impurities increases. Most near-surface soils are nonferromagnetic.
- The permittivity at frequencies above $f > 200$ MHz is proportional to volumetric water content in saturated soils.
- The higher the permittivity, the lower the wave phase velocity.
- The conductivity reflects the availability of hydrated ions. High surface area soils (i.e., clayey soils) and excess salts increase the conductivity of the soil.
- High conductivity reduces the skin depth, which can become shorter than the wavelength.

The application of equations and trends introduced in this section is illustrated in Example 2.

Summary

Elastic and electromagnetic waves provide complementary information about the soil mass in the near-surface. Interrelations between elastic and electromagnetic properties with soil properties highlighted in this review are summarized in Table 8.

In the case of elastic waves, P-waves can be effectively used to verify saturation, and if the soil is saturated, the P-wave velocity can be used to estimate porosity. The S-wave velocity (and the P-wave velocity if the soil is unsaturated, $S_r < 99\%$) reflects the stiffness of the skeleton, which depends on the state of stress, cementation, capillary forces, and soil mass density.

Electromagnetic perturbations provide information about volumetric water content (permittivity at high frequencies), the mobility and availability of ions (electrical conductivity), and the presence of ferromagnetic impurities (magnetic permeability). Permittivity data gathered at low MHz frequencies and conductivity data can be used to infer soil type through surface related effects.

Example 2. Electromagnetic-wave parameter estimation

Consider the same formation as in the previous example for elastic wave properties (sandy soil, saturated $S_r = 1.0$, porosity $n = 0.35$). The saturating fluid is fresh water and the total dissolved salts is TDS = 8 mg/l. Estimate the electromagnetic wave parameters relevant for site characterization with GPR operating with 100 MHz antenna.

Relative magnetic permeability μ

It is assumed that there are no ferromagnetic impurities present

Table 5: $\mu' = 1.0$ $\mu'' = 0.0$

Relative permittivity κ

Table 1: $\theta_v = n \times S_r = 0.35$

Table 6: $\kappa' = 15$ (between 10-to-20) $\kappa'' << \sigma/\omega \times \varepsilon_o$ (assumed)

Effective electrical conductivity σ

Table 7: $\sigma_{el} = 0.15$ TDS $= 1.2 \times 10^{-3}$ S/m

Table 7: $\sigma_{soil} \cong 0.3 \times 10^{-4}$ S/m (estimated with both expressions in the table for $n = 0.35$)

Equation (13) $\sigma_{eff} = \sigma + \kappa'' \times \omega \times \varepsilon_o = 0.3 \times 10^{-4}$ S/m

Wave velocity V_{ph} and wavelength λ

Equation (14) $V_{ph} = 7.75 \times 10^7$ m/s

$\lambda = V_{ph}/f = 0.775$ m

Attenuation α and skin depth S_d

Equation (15) $\alpha = 0.077$ m^{-1}

$S_d = 1/\alpha = 13.0$ m

Table 8. Soil properties and wave parameters.

Wave parameters Soil properties[1]	Elastic wave properties			Electromagnetic wave properties		
	V_P and V_S ($S_r \leq 0.99$)	V_P ($S_r \approx 1$)	α Attenuation	μ^* Permeability	ε^* Permittivity	σ Conductivity
Specific surface S_s Grain size Soil type	Primary (θ and β)		Primary		Primary at f < MHz	Primary
n, e, γ, ρ	± 10%	± 10%	Secondary			Primary
$\theta_v = S_r\, n$					Primary	
S_r (1)	low@high S_r high@low S_r		Primary			Secondary
σ', K_o	Primary		Secondary			
Cementation[2]	Primary		Secondary			
Pore fluid:[1] Ionic concentration	Secondary					Primary
Pore fluid:[1] Polar/nonpolar	Secondary				Primary	
Ferromagnetic inclusions				Primary		

Notes: [1]Affects skeletal stiffness through interparticle forces. [2]Refers to lightly cemented soils.

Symbols: S_S specific surface, n porosity, e void ratio, γ unit weight, ρ mass density, S_r degree of saturation, σ' effective stress, K_o ratio of horizontal to vertical effective stresses, θ and β velocity-stress power relation, V_P P-wave velocity, V_S S-wave velocity, α attenuation coefficient, μ magnetic permeability, ε permittivity, and σ electrical conductivity.

Acknowledgments

The authors' research on wave-based soil characterization has been supported by grants from the national funding agencies, in particular NSF (USA), NSERC (Canada) and CONICET (Argentina).

References

Achenbach, J. D., 1975, Wave propagation in elastic solids: North Holland Publishing Company

Annan, A. P., 1992, Ground penetrating radar: Workshop notes: Sensors and Software.

Archie, G. E., 1942, The electrical resistivity log as an aid in determining some reservoir characteristics: Transactions of the American Institute of Mining, Metallurgical, and Petroleum Engineers, **146**, 54–62.

Arulanandan, K., 1991, Dielectric method for prediction of porosity of saturated soil: ASCE Journal of Geotechnical and Geoenvironmental Engineering, **117**, 319–330.

Cascante, G., and J. C. Santamarina, 1996, Interparticle contact behavior and wave propagation: ASCE Journal of Geotechnical and Geoenvironmental Engineering, **122**, 831–839.

Cho, G. C., and J. C. Santamarina, 2001, Unsaturated particulate materials—Particle level studies: ASCE Journal of Geotechnical and Geoenvironmental Engineering, **127**, 84–96.

Dìaz-Rodrìguez, J. A., and J. C. Santamarina, 2001, Mexico City soil behavior at different strains: Observations and physical interpretation: ASCE Journal of Geotechnical and Geoenvironmental Engineering, **127**, 783–789.

Fredlund, D. G., and H. Rahardjo, 1993, Soil mechanics for unsaturated soils: John Wiley & Sons, Inc.

Göktürk, H. S., T. J. Fiske, and D. M. Kalyon, 1993, Electric and magnetic properties of a thermoplastic elastomer incorporated with ferromagnetic powders: IEEE Transactions on Magnetics, **29**, 4170–4176.

Gucunski, N., and R. D. Woods, 1992. Numerical simulation of the SASW test: Soil Dynamics and Earthquake Engineering, **11**, 213–227.

Hardin, B. O., and V. P. Drnevich, 1972, Shear modulus and damping in soils: Measurement and parameter effects: ASCE Journal of Soil Mechanics, Foundation Division, **98**, 603–624.

Kim, D. S., K. H. Stokoe, and W. R. Hudson, 1991. Deformational characteristics of soils at small to intermediate strains from cyclic tests: Report 1177–3, Center for Transportation Research, Bureau of Engineering Research, University of Texas, Austin.

Kim, T. C., and M. Novak, 1981, Dynamic properties of some cohesive soils of Ontario: Canadian Geotechnical Journal, **18**, 371–389.

Kjartansson, E., 1979, Constant Q-wave propagation and attenuation: Journal of Geophysical Research, **84**, 4737–4748.

Klein, K., and J. C. Santamarina, 2000, Ferromagnetic inclusions in geomaterials—Implications: ASCE Journal of Geotechnical and Geoenvironmental Engineering, **162**, 167–179.

Kokusho, T., 1980, Cyclic triaxial test of dynamic soil properties for wide strain range: Soils and Foundations, **20**, 45–60.

Kokusho, T., Y. Yoshida, and Y. Esashi, 1982, Dynamic properties of soft clay for wide strain range: Soils and Foundations, **22**, 1–18.

Laird, J. P., and K. H. Stokoe, 1993, Dynamic properties of remolded and undisturbed soil samples tested at high confining pressures: Geotechnical Engineering Report GR93-6, Electrical Power Research Institute.

Lanzo, G., and M. Vucetic, 1999. Effect of soil plasticity on damping ratio at small cyclic strains: Soils and Foundations, **39**, 131–141.

Li, X. S., W. L. Yang, C. K. Shen, and W. C. Wang, 1998, Energy-injecting virtual mass resonant column system: Journal of Geotechnical and Geoenvironmental Engineering, **124**, 428–438.

Miller, R.D., J. Xia, C. B. Park, and J. Ivanov, 1999, Multichannel analysis of surface waves to map bedrock: The Leading Edge, **18**, 1392–1396.

Mitchell, J. K., 1993, Fundamentals of soil behavior, Second Edition: John Wiley & Sons, Inc.

O'Konski, C. T., 1960, Electrical properties of macromolecules V. Theory of ionic polarization in polyelectrolytes: Journal of Physical Chemistry, **64**, 605–618.

Olhoeft, G. R., 1981, Electrical properties of rocks: Chapter 9, Physical Properties of Rocks and Minerals, McGraw Hill/CINDAS Data Series on Material Properties, McGraw-Hill Book Co., 257–329.

Parkhomenko, E. I., 1967, Electrical properties of rocks, Plenum Press.

Peplinski, N. R., F. T. Ulaby, and M. C. Dobson, 1995, Dielectric properties of soils in the 0.3–1.3 GHz range: IEEE Transactions on Geoscience and Remote Sensing, **33**, 803–807.

Reynolds, J. M., 1997, An introduction to applied and environmental geophysics: John Wiley & Sons, Inc.

Richart, F. E., J. R. Hall, and R. D. Woods, 1970, Vibrations of soils and foundations: Prentice-Hall Inc.

Rix, G. J., G. L. Hebeler, and M. C. Orozco, 2002, Near-surface V_s profiling in the New Madrid seismic zone using surface wave methods: Seismological Research Letters, **73**, 380–392.

Saarenketo, T., 1998, Electrical properties of water in clay and silty soils: Journal of Applied Geophysics, **40**, 73–88.

Santamarina, J. C., and G. Cascante, 1996, Stress anisotropy and wave propagation: A micromechanical view: Canadian Geotechnical Journal, **33**, 770–782.

Santamarina, J. C., K. A. Klein, and M. A. Fam, 2001, Soils and waves: John Wiley & Sons, Inc.

Selig, E. T., and S. Mansukhani, 1975, Relationship of soil moisture to the dielectric property: Journal of the Geotechnical Engineering Division, **101**, 757–770.

Stokoe, K.H. II, S. G. Wright, J. Bay, and J. Roësset, 1994, Characterization of geotechnical sites by SASW method, *in* R. D. Woods, ed., Geophysical characterization of sites. New Delhi Oxford & IBH Publishing Co. Pvt. Ltd., 15–25.

Tokimatsu, K., 1995, Geotechnical site characterization using surface waves, *in* K. Ishihara, ed., Earthquake geotechnical engineering: A. A. Balkema, 1333–1368.

Topp, G. C., J. L. Davis, W. G. Bailey, and W. D. Zebchuk, 1980, The measurement of soil water content using a portable TDR hand probe: Canadian Journal of Soil Science, **64**, 313–321.

Wang, J. R., 1980, The dielectric properties of soil-water mixtures at microwave frequencies: Radio Science, **15**, 977–985.

Wensink, W. A., 1993, Dielectric properties of wet soils in the frequency range 1–3000 MHz: Geophysical Prospecting, **41**, 671–696.

White, J. E., 1983, Underground sound: Elsevier Science Publishing Company, Inc.

Yasuda, N., and N. Matsumoto, 1993. Dynamic deformation characteristics of sand and rockfill materials: Canadian Geotechnical Journal, **30**, 747–757.